PHYSICAL REVIEW B VOLUME 15, NUMBER 3 1 FEBRUARY 1977

Mobility of electrons on the surface of liquid helium*

Frank Bridges† and J. F. McGill‡
Division of Natural Sciences, University of California at Santa Cruz, Santa Cruz, California 95064
(Received 28 June 1976)

A time-of-flight mobility measurement ($1.17 < T < 2.7$ K) is made on low-density electron pulses ($n < 10^4$ cm^{-1}) moving above the surface of liquid helium with the electrons constrained against the liquid surface by a net dc electric field. Below 1.45 K the mobility starts to level off in the manner predicted by Cole although at the lowest temperatures the experimental value is slightly higher than Cole's value. This is direct evidence that the electron-ripplon interaction is important at these temperatures. The mobility at high drift fields is also reported.

I. INTRODUCTION

Electrons on the surface of liquid helium form a two-dimensional system that has attracted the attention of both theorists and experimentalists. The surface of this system is unusually clean, with the major defect being only a few ^{3}He impurities on the surface, and one might therefore expect that first-order theoretical calculations[1,2] would give a fairly good approximation to the main experimental features. By and large this has proved true. The spectroscopic data of Grimes and Brown[3] agree fairly well with the theoretical model of Cole,[2] and the experimental determination of the splittings between the lower electronic surface states differ only about 5% from the theoretical values. However, one type of experiment—the investigation of the electron mobility—has not given complete agreement with theory in previous work.[4-7] Cole[8] has outlined the earlier investigations, both theoretical and experimental, in a recent review article.

The main scattering mechanisms[2,9] which determine the mobility are electron–vapor-atom scattering and electron-ripplon (quantized surface waves) scattering; with the latter only being important for the lower-energy surface states. Since the vapor density, and hence the strength of the electron-vapor-atom scattering mechanism, decreases exponentially with temperature, one expects that eventually at low enough temperatures, electron-ripplon scattering should dominate. Using a simple model for the electron-liquid polarization potential, Cole[2] calculated the temperature dependence of the mobility and estimated that the latter interaction should become dominant below 1 K. However, none of the earlier work[4-7] gave any evidence for a ripplon-limited mobility at this temperature.

Recently, Grimes and Adams[10] investigated the plasma resonance in this system at relatively high-electron densities. From the linewidth of the resonance line they inferred a ripplon-limited temperature-independent ac mobility, for $T < 0.68$ K, that is nearly two orders of magnitude higher than the theoretical prediction of Cole. Some attempts have been made to explain these results,[11] but a model which gives both the correct order of magnitude for μ and also predicts the temperature independence of the ripplon-limit mobility observed in this experiment is not yet available.

A ripplon-limited mobility has also been observed by Rybalko *et al.*,[12] by measuring ac losses at 2.98 and 14.65 MHz. Their values of the mobility lie a factor of 5 below the results of Grimes and Adams and nearly an order of magnitude above Cole's predictions. Further, between 0.5 and 0.9 K there is a weak T^{-1} temperature dependence which is not theoretically predicted by any models[2,11] at present.

We have now measured the mobility μ of electrons moving along a helium surface between 1.2 and 2.7 K, using a *direct time-of-flight method*.[13] In this experiment, which uses very *low-electron densities* and *small drift fields*, we have observed a leveling off of the mobility, starting near 1.4 K, which we interpret as the predicted onset of ripplon-limited scattering. The general form of the data agrees with the theoretical prediction of Cole,[8] although our limiting value of the mobility is higher.

The interpretation of our results depends on the theoretical understanding of this two-dimensional system, and the relevant theoretical background which pertains to mobility measurements is presented in Sec. II. A discussion of several assumptions which are incorporated in the theory is included here.

In Sec. III we discuss the previous experiments in which a search was made for a ripplon-limited mobility. Our experimental method and apparatus, including a list of constraints which arise from assumptions in the theory, are given in Sec. IV, and the new experimental results are presented in Sec.

V. The conclusions and a discussion of the discrepancies between various experiments are given in Sec. VI.

II. THEORETICAL BACKGROUND

A. Surface states

The electronic surface states of electrons above the surface of liquid helium (and other dielectrics) have been extensively studied by several investigators in the past few years. Here we present the main features of these works.[1,2,9] An electron moving above the surface of liquid helium experiences an attractive interaction towards the surface which results from the small dielectric polarizability of helium. For electrons far above an infinite flat liquid surface, this interaction is well described by the classical potential

$$V=-Qe^2/z, \quad Q=\tfrac{1}{4}(\epsilon-1)/(\epsilon+1). \tag{1}$$

Here ϵ is the dielectric constant of the liquid (ϵ for the vapor is taken to be 1.000) and z is the vertical distance above the interface. For small z, the detailed structure of the surface—lack of definition of the interface, atomic nature of the liquid, etc.—becomes important and the potential differs from the classical expression when z is less than some value b of order 3–4 Å. The potential for $0<z<b$ is not known exactly and has been approximated in several ways. Cole[8] used a constant square-well potential for $0<z<b$, while Grimes and Brown[3] proposed a potential of the form $(z+b)^{-1}$. However, the actual form near the surface is likely better described by the potential of Huang *et al.*[14]

At the surface ($z=0$), electrons experience a strong repulsive barrier which is primarily the result of the exclusion principle. Experimentally, this potential barrier has a height of approximately 1 eV.[15] In the models of Cole[8] and Grimes and Brown,[3] this barrier is represented by a step function at (or near) the surface, while in the potential of Huang *et al.*,[14] a rapid increase in the potential occurs over a few angstroms. As will become apparent shortly, the form of the potential *at the surface* is important for investigations of the electron-ripplon interaction on liquid helium.

The net result of these two interactions is a shallow potential well, as indicated schematically in Fig. 1. Using a step-function approximation of height V_0 for the surface-potential barrier, the eigenfunctions and energy levels of the bound states can be calculated in the noninteracting single-particle approximation. In this solution, the wave functions have the form

$$\psi_{k,l}(\vec{r})=A^{-1/2}\exp(i\vec{k}\cdot\vec{\rho})\Phi_l(z), \tag{2}$$

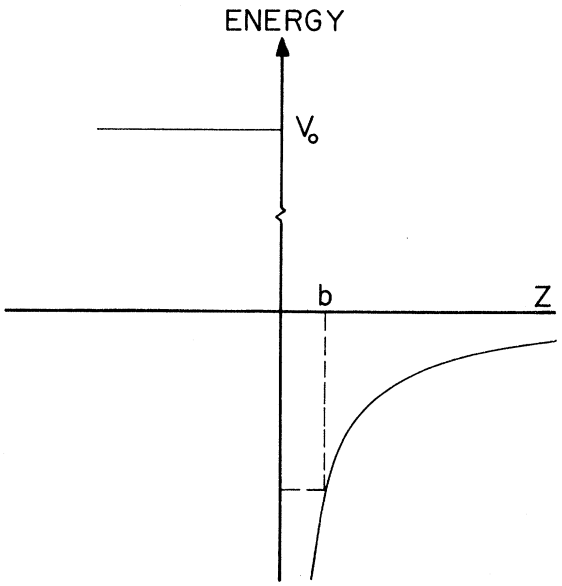

FIG. 1. Schematic representation of the potential seen by an electron near the free surface of ^{4}He. The liquid surface is in the plane $Z=0$.

where $\vec{\rho}$ is the component of $\vec{r}$ along the surface (the x,y plane), $\vec{k}$ is the electron wave vector, and A is the surface area. The functions Φ_l are very similar to the radial s-wave hydrogenic functions $rR(r)$ and deviate from these functions primarily when $z<b$. In the limit $b\to 0$, $V_0\to\infty$ these functions are exactly the hydrogenic functions.

The energy is given by[8]

$$E_l(k)=E_{\perp l}+E_{\parallel}=E_{\perp l}+\hbar^2k^2/2m, \tag{3}$$

where $E_{\perp l}$ is the eigenenergy of Φ_l and m is the electron mass. In the hydrogenic limit, $E_{\perp l}$ becomes

$$E_{\perp l}=-Q^2e^2/2a_0l^2, \tag{4}$$

with a_0 the usual Bohr radius.

B. Mobility of electrons on the surface of liquid helium

1. Ohmic regime

The mobility of electrons moving in two dimensions on the surface of helium has been investigated theoretically by Cole,[8] Crandall,[16] and Shikin.[9] In the Ohmic regime, the drift velocity v_D is proportional to the drift field F_D, parallel to the surface, and the mobility μ, defined by v_D/F_D, is independent of the electric field. At low-electron densities, for which electron-electron interactions are assumed to be negligible, the main mechanisms which determine the mobility are electron–vapor-atom and electron-rip-

plon scattering, and the momentum transfer rates which result from these scattering processes are denoted λ_v and λ_r, respectively. Once these functions are known, the two-dimensional mobility μ may be calculated from the expression[8]

$$\mu(T) = \frac{e}{m} \int_0^\infty dk\, k^3 \lambda^{-1} e^{-\beta E_{\parallel}} \Big/ \int_0^\infty dk\, k^3 e^{-\beta E_{\parallel}} . \quad (5)$$

Here e is the charge of the electron and $\beta = (kT)^{-1}$.

At high temperatures where the density of vapor atoms is large, vapor-atom scattering dominates. Cole[2] has calculated the momentum transfer rate for this process under the assumption that *all electrons are in the ground hydrogeniclike state and obtained*

$$\lambda_v = 3\pi^2 n_v a_s^2 \hbar q_0 / 4m , \quad (6)$$

where n_v is the vapor density, a_s is the scattering length ($a_s = 0.61$ Å for He), and $q_0 = 2Q/a_0$. As the temperature is lowered, the vapor density drops exponentially with temperature and the mobility consequently increases rapidly. Eventually, however, the electron–vapor-atom scattering process becomes slow enough that the electron-ripplon scattering interaction becomes important and at very low temperatures the latter mechanism dominates. From theoretical considerations this crossover is expected to occur near 1 K.

The momentum transfer rate for electron-ripplon scattering (in the absence of external fields) was first calculated by Cole,[2] using a perturbation approach and two-dimensional plane-wave electron states. For electrons in the ground hydrogenic state, he obtained, to lowest order,

$$\lambda_{r0} = m\pi^2 c^2 q_0^4 / 8\hbar^3 \sigma \beta k^2 , \quad (7)$$

where c is the interaction coupling constant ($c = Qe^2/\pi$), and σ is the surface tension of helium. This expression, however, neglects an effective short-range interaction at the liquid-vapor interface. Using an adiabatic approximation for the electron states and an infinite potential barrier at the surface, Shikin and Monarkha[17] suggest that the surface matrix element cancels that obtained by Cole. Subsequently, Gaspari and Bridges[18] considered a reformulation of the scattering problem which includes the short-range interaction due to vertical shifts of the liquid surface. They then found that to first order, the total scattering matrix element is the difference of two terms; one identical with the main matrix element obtained by Cole[2] and a surface term of the *opposite* sign. For the finite barrier, the ratio R of the magnitude of Cole's matrix element to that of the surface term depends sensitively on the details of the potential near the interface. Using Cole's potential model with a 1-eV potential barrier at the surface, one finds that R ranges from 2 to 10 for reasonable values of the parameter b ($1 < b < 4$ Å). However, for an *infinite* potential barrier (and b within this range), $R = 1$, the first-order matrix element is negligibly small, and the net result reduces to that of Shikin and Monarkha.[17]

Including the surface term in the scattering matrix element modifies Cole's result for λ_r slightly

$$\lambda_r^{-1} = \lambda_{r0}^{-1}(1 - 1/R)^{-2} . \quad (8)$$

As indicated above, the value of R depends sensitively on the details of the potential well at the liquid surface and cannot be estimated accurately with the present crude theoretical models. On the other hand, a measure of R should give new information about the shape of the potential at the surface.

The mobility calculated from λ_r above is found to be almost independent of temperature as a result of the particular energy and temperature dependence of λ_{r0} [Eq. (7)]. This leads to a nearly temperature-independent mobility at low temperatures whenever electron-ripplon scattering dominates. (The very weak temperature dependence remaining in μ is the result of the slight dependence of the surface tension on temperature.[19,20]) This predicted "leveling off" of the mobility at low temperatures ($T < 1$ K) characterizes the electron-ripplon scattering regime, and the search for this effect has been the object of many earlier investigations.[4-7,10,12]

Yet another contribution to electron-ripplon scattering should appear if a large electric field $F_\perp$ presses the electrons against the surface.[7,9,17,21] This additional interaction appears to be important when $F_\perp > 100$–300 V/cm. At the low holding field used in our experiment ($F_\perp = 20$ V/cm), the effect should be negligible and will not be considered further.

An experimental observation of the theoretical ripplon-limited mobility considered above depends on a number of assumptions in the theory being satisfied by the experimental situation. We discuss three questions which appear to be important in mobility studies. (i) Is the surface charge density small enough that electron-electron effects can be neglected? (ii) Is the plane-wave assumption a good approximation for the experimental situation? (iii) Are all (or most) of the electrons in the ground hydrogenic state? These questions are in some ways interconnected.

The questions concerning the charge density at which the electron-electron interactions become important for mobility studies are difficult to answer. Crandall and Williams[22] have suggested that under some conditions the electron-electron interaction may be such that a two-dimensional

electron Wigner crystal can form. If this occurs, the electron-electron interaction is obviously very important and the plane-wave assumption is no longer valid. The densities and temperatures at which such a crystallization should occur have been studied by several investigators. Crandall[23] estimated the melting curve as a function of electron density and temperature by considering the ratio $\alpha = \langle u^2 \rangle / R_0^2$, where $\langle u^2 \rangle$ is the average square displacement about a lattice site, and R_0 is the lattice parameter. From the resulting phase diagram (for a square crystal lattice), the critical density for crystallization at 1 K lies above 10^6 cm^{-2} and is possibly greater than 10^7 cm^{-2}. Platzman and Fukuyama[24] obtained the phase diagram of a triangular electron lattice by considering the ratio Γ_0 of the potential energy to the kinetic energy. In the high-temperature nondegenerate regime, which is the region of interest here, the critical density along the melting curve is given by[24]

$$n_c = (kT\Gamma_0/\pi^{1/2}e^2)^2 . \tag{9}$$

Using a microscopic theory, they[24] estimate $\Gamma_0 \simeq 2.8$ and hence at 1 K, $n_c \simeq 10^6$ cm^{-2}. Thus, both theoretical estimates suggest that at electron concentrations near 10^6 cm^{-2}, the electron-electron interaction is important and crystallization of the electrons is possibly occuring. On the other hand a computer simulation of a two-dimensional electron gas by Hockney and Brown,[25] which includes only Coulomb interactions between the electrons, indicates that the potential energy must be much larger than the kinetic energy ($\Gamma_0 \simeq 95$) before crystallization actually occurs. However, partial localization of the electrons as a result of the Coulomb interaction certainly occurs for much smaller values of Γ_0. Even at $\Gamma_0 = 1 (n_c \simeq 10^5/\text{cm}^2)$ it is quite possible that the electron-electron interaction cannot be neglected in mobility studies and the assumption of a noninteracting gas may not be valid. We suggest, therefore, that if the free-electron model is to be a valid approximation, n probably must be less than 10^6 cm^{-2} and likely less than 10^5 cm^{-2}.

The question of the occupation of the hydrogenic-like ground state can be answered easily if no external fields are present. Then at 1 K only a few percent of the electrons will occupy the ground state[2,8,26] even though the binding energy is 10 K. This is strictly a density-of-states effect. The energy levels of the hydrogenic states [Eq. (4)] become closer and closer together as the electron energy is increased towards zero (continuum) and the density of states increases rapidly. Only at temperatures below 0.5 K is the Boltzman factor large enough to overcome the large density of states of the higher quantum levels.[8] Fortunately, this difficulty can easily be eliminated by the application of a small electric field $F_\perp$ perpendicular to the surface. Such a field spreads out the high quantum-number states, thereby greatly reducing the density of states at energies near zero. With an applied field of several V/cm, most of the electrons should be in the ground state. Also, such small fields on the order of 10–20 V/cm should have a negligible effect on the mobility calculated for the ground hydrogenic state.[9]

2. *Non-Ohmic regime—hot electrons*

At high drift fields, the drift velocity is no longer a linear function of field and μ becomes a function of F_D. Such behavior is well known in semiconductors and has recently been considered for the two-dimensional electron gas on liquid helium by Crandall.[27,28] In this regime, the electrons gain appreciable energy from the electric field and the average energy per electron is greater than kT. Such electrons are termed hot electrons. As in the Ohmic case, two scattering mechanisms contribute to the electron mobility.

a. Vapor-atom scattering. The momentum transfer rate for vapor-atom scattering of electrons in the hydrogenic ground state [Eq. (6)] is independent of energy and hence an increase of the average electron energy should not change the mobility if the electrons remain in this state. However, as the energy in the plane-wave states increases, the likelihood of scattering into the upper hydrogenic states also increases and the upper levels become populated. Vapor-atom scattering of electrons in these excited states then becomes the determining factor for the mobility. In a recent paper, Crandall[28] considered this process in detail. He found that although the scattering cross section decreases for the higher quantum states, the total relaxation rate actually increases and hence the *mobility decreases*. This result is another density-of-states effect. As the electrons move to higher excited levels, the electrons can scatter into more and more final states. The density of states is found to increase faster than the decrease in the scattering cross section, and thus leads to a net decrease in mobility. The theoretical curves obtained by Crandall[28] are presented with the experimental data.

b. Ripplon scattering. The momentum transfer rate for this process [Eq. (7)] varies inversely with energy for electrons in the ground state. Therefore, as the average energy rises, the mobility will also increase. Of course, this assumes that only the lowest state is occupied. If, as a result of heating, the electrons scatter into higher

quantum states, the ripplon-limited mobility becomes even larger since electrons in the excited states are far from the surface and have a weaker coupling to the ripplons.

In the intermediate region where both vapor-atom scattering and ripplon scattering are present, two competing effects are present; an increase in μ at high drift fields from the ripplon contribution and a corresponding decrease in μ from the vapor-atom scattering component. It is expected that as the drift field increases, the mobility will first increase above the Ohmic value and then decrease as the vapor-atom scattering process starts to dominate.[28] How large the resulting "bump" in the mobility curve is, depends sensitively on the relative magnitudes of the two momentum-transfer rates and on the energy dependencies of these processes. For the ripplon process, higher-order terms which are energy dependent may become important; how important, has yet to be determined. However, it is likely that further theoretical work will be necessary before a detailed calculation of the shape and size of this bump is available.

III. PREVIOUS EXPERIMENTS

A number of ingenious experiments have been devised to look for evidence of electron surface states on liquid helium. Primarily, three different methods have been applied: a direct measure of the lifetime of electronic states on a liquid helium surface[26,29]; the measurement, by several techniques, of the mobility of electrons moving across the surface,[4-7,12] measurements of the momentum-relaxation time[10]; and a spectroscopic-absorption measurement of direct transitions between the hydrogeniclike states.[3] The latter experiment indicated conclusively the existence of surface states although small discrepancies with the available models still remain.

The mobility measurements, however, have been inconclusive concerning the existence of surface states[4-7] or disagree[10,12] considerably with the theoretical estimates, although they generally agree on the two dimensionality of the electron gas on a helium surface. The mobilities measured are all lower than the theoretical curve for three-dimensional gas-atom scattering and for $T > 1$ K are generally near or below the theoretical results for a two-dimensional gas. Several of the early mobility investigations were made before the importance of the density-of-states factor was appreciated,[8] and before estimates of the critical density for possible crystallization were available. Thus, the constraints imposed by these considerations were not included in some experiments.

One of the first measurements, by Sommer and Tanner,[5] employed one electrode above the surface and three below. These electrodes provided a vertical holding field for the electron gas. A sine wave was applied to one of the outer submerged electrodes and an induced signal on the other outer electrode was detected. The two electrodes were coupled via the surface-charge density, and the resulting phase lag between the input and detected signals was a measure of the mobility. Although very sensitive, this method is indirect and suffers from the need of an accurate model to relate the phase shift to the mobility.

The results of this experiment are shown in Fig. 2 along with other experimental data. The data of Sommer and Tanner are lower than all other data and, more importantly, show no leveling off of the mobility at low temperatures. A possible reason for not seeing the predicted ripplon-limited value arises from the fact that a fully charged surface was used with the electron source usually operated continuously. At the large-holding fields used (>40 V/cm), charge densities in excess of 10^7 cm^{-2} were present, which suggest that in these measurements the electron-electron interaction was not negligible and that possibly some crystallization may have occurred (see Sec. IIB1).

Ostermeier and Schwarz[4] used a time-of-flight method to measure the mobility directly but observed no evidence for a ripplon-limited mobility over the range of parameters available with their apparatus. Unfortunately, their mobility cell

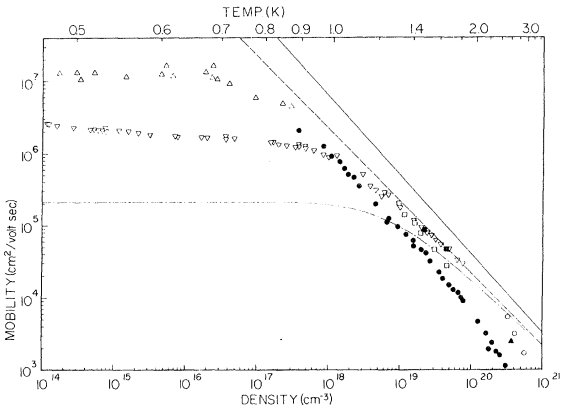

FIG. 2. Plot of mobility vs vapor density showing theoretical curves and results of previous experiments. The solid line is from three-dimensional kinetic theory. The straight-dashed line is from two-dimensional kinetic theory. The curved dashed line includes ripplon and two-dimensional vapor scattering (Ref. 8). Δ, Grimes and Adams (Ref. 10); ∇, Rybalko *et al.* (Ref. 12); ▲, Ostermeier and Schwarz (Ref. 4); ●, Sommer and Tanner (Ref. 5); ○, Levine and Sanders (Ref. 34); □, Brown and Grimes (Ref. 6); ■, Rybalko and Kovdrya (Ref. 7).

could not operate at very-low-drift electric fields ($F_D \geq 0.3$ V/cm), and they were consequently unable to obtain data in the linear regime below 1.9 K. At higher temperatures their results in the high-drift field regime showed that the mobility eventually decreases with increasing drift field, and were the first reported data of hot electrons on liquid helium.

In these time-of-flight experiments,[4] an additional problem was the lack of a sizable holding field. Measurements were taken with no holding field or a holding field which was much less than the drift field. Consequently, the net population of electrons which remained in the ground state was likely to be very small. The new experiments we have made are essentially extensions of this time-of-flight method to include much smaller drift fields and larger holding fields.

Rybalko and Kovdrya[7] have also used the time-of-flight method to investigate the electron mobility on a helium surface (Fig. 2). These investigators concentrated on the effects at very high holding fields and found evidence of slow-moving groups of electrons at high-surface charge densities and large perpendicular fields ($F_\perp > 300$ V/cm). Their data at low or zero holding fields only cover the temperature range of 1.4–2.0 K, and generally agrees with the calculation for vapor-atom scattering of a two-dimensional electron gas. These results, however, do not extend to low enough temperatures to test for ripplon scattering in the regime where the ripplon-limited mobility is independent of $F_\perp$.

Another determination of the surface mobility was obtained from the cyclotron resonance experiment of Brown and Grimes.[6] The linewidth of the absorption line is determined by the scattering time, and hence is related to the mobility. These data agree qualitatively (Fig. 2) with the calculation for electron–vapor-atom scattering in a two-dimensional gas, but (within their errors) do not extend to low enough temperatures and densities to check for ripplon scattering. In addition, these experiments used large charge densities (10^5–10^6 cm^{-2}) and the electron-electron interaction would be an important consideration in extending this method to lower densities.

In a recent letter, Grimes and Adams[10] reported studies of the plasma resonance for this two-dimensional electron system over the temperature range $0.5 < T < 0.9$ K. Assuming that the width of their resonance line is determined by the momentum relaxation scattering time τ_r, they calculate an ac mobility ($\mu = e\tau_r/m$) that is essentially independent of T and vapor density below 0.68 K, but surprisingly is much larger than our results and the earlier predictions of Cole (see Fig. 2). Platzman and Beni have attempted to explain the magnitude of the observed mobility using Shikin's matrix element which is identical to the infinite-barrier case of Ref. 18. The residual interaction which remains leads to a ripplon-limited mobility that varies as T^{-2}. Although in the limit of small holding fields, the magnitude of μ from this model is about right at $T = 0.5$ K, the lack of any temperature effects between 0.48 and 0.68 K in the experimental data[30] (whereas a T^{-2} dependence would give a change by a factor of 2) indicates that the theoretical understanding of the mobility is still incomplete. It should, of course, be understood that in these experiments,[10] the plasma lifetime is the measured quantity, whereas in the present experiments the drift velocity is measured. These are not necessarily equivalent physical situations.

The large value of the ripplon mobility and the disagreement with the existing theory may also arise from the high densities of electrons used in these experiments ($10^6 < n < 10^9$ electrons/cm^2). Clearly, the use of the free-electron model is questionable at these densities.

Finally, Rybalko *et al.*,[12] investigated the power absorption of electrons on the surface of liquid helium at 2.98 and 14.65 MHz. From these measurements they obtained a mobility μ which clearly begins to level off below 1 K (Fig. 2). However instead of approaching a constant value, a weak T^{-1} temperature dependence is observed from 0.5 to 0.9 K. In addition the magnitude of the mobility in their measurements is about midway between the temperature-independent values of Grimes and Adams[10] and the limiting value which our data is approaching.

The reason for the disagreement between these results and theory[2,11] is not clear but may also arise from the high density of surface electrons $n \simeq 10^5$–10^6 electrons/cm^2. A further discussion of this and other previous data will be included in Sec. VI.

IV. EXPERIMENTAL CONSIDERATIONS

A. Constraints

In Sec. II, several of the assumptions used in the theoretical developments were discussed. To meet these assumptions, the design of the apparatus was constrained by the following conditions.

(i) A holding field ($F_\perp$), perpendicular to the surface, must be present to populate the lowest hydrogenic level.[8] For $F_\perp$ in the range 1–20 V/cm, the field is large enough to depopulate the excited states yet small enough that the additional contribution to electron-ripplon scattering, which varies as $F_\perp^{-2}$, is not important.[9]

(ii) The surface-charge density should be kept low enough that the neglect of electron-electron interactions and the assumption of plane wave electron states are valid approximations. From Sec. II, electron densities less than 10^5 cm^{-2} should meet this restriction. In pulse measurements, however, a further restriction on the charge density is imposed by the requirement that the spreading field at the edge of the charge distribution is small compared to the drift field. To satisfy this criterion for a disk of charge 0.2 cm in diameter, we adopted the stronger conditions $n < 10^4$ cm^{-2}.

(iii) Small drift fields must be used to minimize heating effects and permit data to be taken in the linear regime.

B. Mobility cell

The experimental cell for our time-of-flight measurements is a parallel plate capacitor, fabricated from X-band waveguide (Fig. 3). One plate sits in the liquid helium and the other in the vapor above the free surface. With the capacitor charged to some potential by a battery, an electric field exists between the plates. By tipping the capacitor with respect to the liquid surface, field components parallel and perpendicular to the surface can be obtained. If the ratio of plate length to separation is large enough, there is a region in the center of the cell where fringe effects are negligible,[31] and the field components along the axis of the cell are related by $F_D \simeq \theta F_\perp$, where θ is the tilt angle of the plates with respect to the surface ($\theta < 3°$), F_D is the field component along the surface, and $F_\perp$ the component normal to the surface. For the small angles used in this experiment, $F_\perp$ is taken to be equal to the applied electric field.

Electron pulses are injected into the field region through two 0.2-cm-diam holes (drilled into the top plate of the capacitor) and follow the field lines to the surface of the helium. Most electrons do not penetrate the surface barrier, and are constrained to move along the surface under the influence of the field component F_D parallel to it. To ensure that the electrons move along the central axis of the cell, side walls (Fig. 3) are included which are connected to the top plate. At the end of the cell, the electron pulse is collected by a grid and collector plate assembly.

Considerable care was taken to make the drift field in the cell as uniform as possible. Since the end fringe fields arising from the grid and collector plate assembly could be quite large in general, several steps were taken to eliminate this potential problem. First, the end effects were minimized by fabricating the grids in a voltage-divider arrangement. Each grid consisted of four equally spaced gold-plated brass wires, coupled together

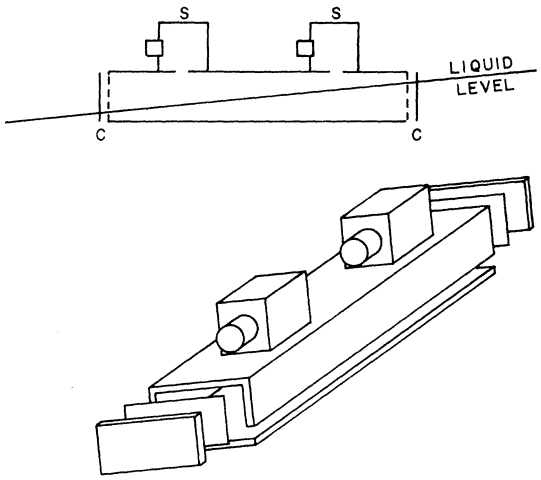

FIG. 3. Schematic of the experimental cell, showing top and bottom plates, grids, collector plates (c) and radioactive electron sources (s).

by resistors, such that the voltage drop from wire to wire was identical to the potential drop for an equivalent displacement within the cell. Then, the remaining end effect was eliminated by measuring the time-of-flight of the electrons for two different path lengths. The electrons from one source (near source) traverse primarily the fringe field region while electrons from the other source (far source) traverse the center region of the cell, where the field is uniform,[31] as well as the fringe region. The time delay t between the gating of the electron source and the detection of the output pulse is the time-of-flight for the electrons. The difference in t for the two electron sources (Δt) is a measure of the time for electrons to traverse the center region where fringe effects are negligible. In practice, Δt is measured for several different values of drift field, and the drift velocity $v_D = L/\Delta t$ is plotted as a function of the drift field along the surface ($L = 3.9$ cm is the length of the central drift region). The slope of such a plot is the mobility.

The cell is bisymmetric with a grid, collector plate, and electron source at each end. In this configuration, the apparatus can be accurately leveled by measuring transit times for electrons moving in either direction along the axis of the cell. As discussed above, the component of the applied electric field along the helium surface was obtained by tipping the cell through a small angle θ. This technique was found to be useful for angles down to $\pm 2 \times 10^{-3}$ rad. Below this value, sloshing modes of the liquid surface caused pulse broadening which prevented an accurate determination of the transit time (see Sec. IV D). Thus, with a 20-V/cm perpendicular field, the smallest useful

drift field was 40 mV/cm, comparable to the ac fields used in Refs. 5 and 10. At these small drift fields, electron heating was not a problem in the temperature range over which measurements were made (see Sec. V B).

Two types of pulsed electron sources were used in the course of the experiment—cold cathode emitters and radioactive (^{210}Po) sources. Much of the lower-temperatures data were taken with the radioactive sources which proved to be a convenient means of obtaining low-density electron pulses. The details of this source are shown in Fig. 4. A partially collimated α source (^{210}Po) is mounted in the side wall of a small brass box situated above an injection hole of the mobility cell (Fig. 3). Emerging α-particles ionize some of the helium vapor, producing a few free electrons. These electrons are restricted from entering the capacitor cell by a small positive potential (+1 V) applied between the box and the top plate. Injection of an electron pulse is achieved by applying a large negative pulse (typically −10 V) to the box. Varying the height and width of this pulse controls the number of ejected electrons. In addition, the side mounting of the α source was designed in such a way that α-particles could not pass directly through the injection hole into the cell. This insured that unwanted electrons were not generated inside the capacitor region.

C. Other equipment

The pulse-detection system is a fast electrometer with the input stage [a MOSFET (metal-oxide-semiconductor field-effect transistor) source follower and a 10^7-Ω input resistor] operating in the liquid-helium bath. The current sensitivity is about 0.5 fA/(Hz)$^{1/2}$, and the electrometer can detect 10^{-13} A in a 50-μsec pulse or 30 electrons/50-μsec pulse. The pulses were averaged using a PAR TDH-9 Waveform Eductor to obtain a good

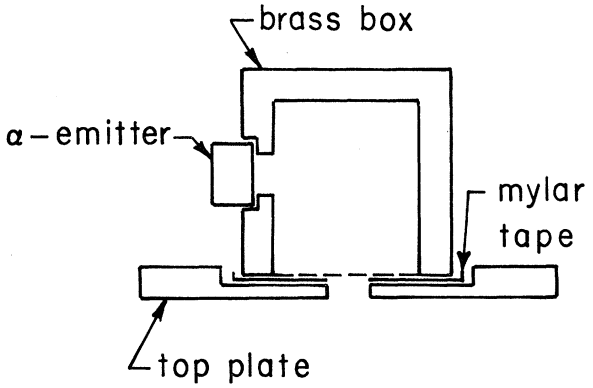

FIG. 4. Cross-section schematic of pulsed radioactive electron source.

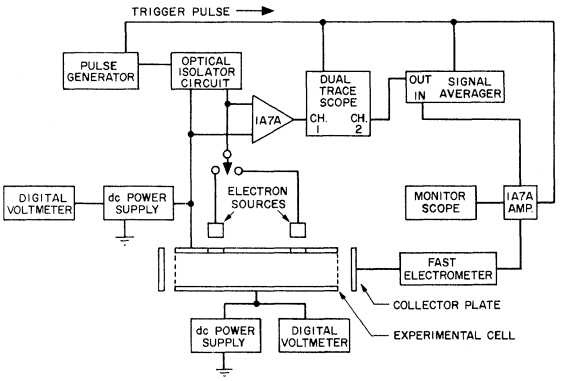

FIG. 5. Schematic of the apparatus and electronics.

$S/N(S/N \geq 25)$. This typically required 10^3–10^4 pulses. With this system, transit times from 30 μsec to 0.5 sec have been measured.

A schematic of the experimental arrangement is shown in Fig. 5. The floating voltage between the capacitor plates was usually set at 20 V/cm but could be varied from 10 to 100 V. The voltage between the collector plates (which operated at ground potential) and the lower plate was typically 10 V. All voltage supplies were battery operated.

The cryostat used in these experiments was of standard design but was mounted on vibration isolation pads to minimize the effects of sloshing modes in the liquid helium. Isolation was also included in the pumping line to eliminate vibrations from the pump. The temperature of the helium bath was electronically controlled and could be regulated to 5×10^{-4} K.

D. Shape and analysis of the pulses

1. Input pulse

Pulses of electrons are placed on the helium surface by pulsing the radioactive sources for a short time, typically 50 or 100 μsec. During this time, those electrons already on the surface are moving at the drift velocity away from the source. For typical velocities of order 2×10^4 cm/sec and a pulse length of 50 μsec this leads to a clump of charge that is spatially spread over 1 cm and whose charge density ρ is approximately trapezoidal in shape as shown in Fig. 6(a). This shape, rather than that of a rectangular pulse, arises from the finite extend of the injection hole (0.2 cm) and the ramp section of the pulse extends for 0.2 cm.[32] This pulse of electrons leads to a current pulse ρv_D of the same shape.

A typical pulse consists of 30–600 electrons. Assuming the width of the charge distribution is about 0.2 cm, then the space charge field component near the leading or tail end of the pulse is of

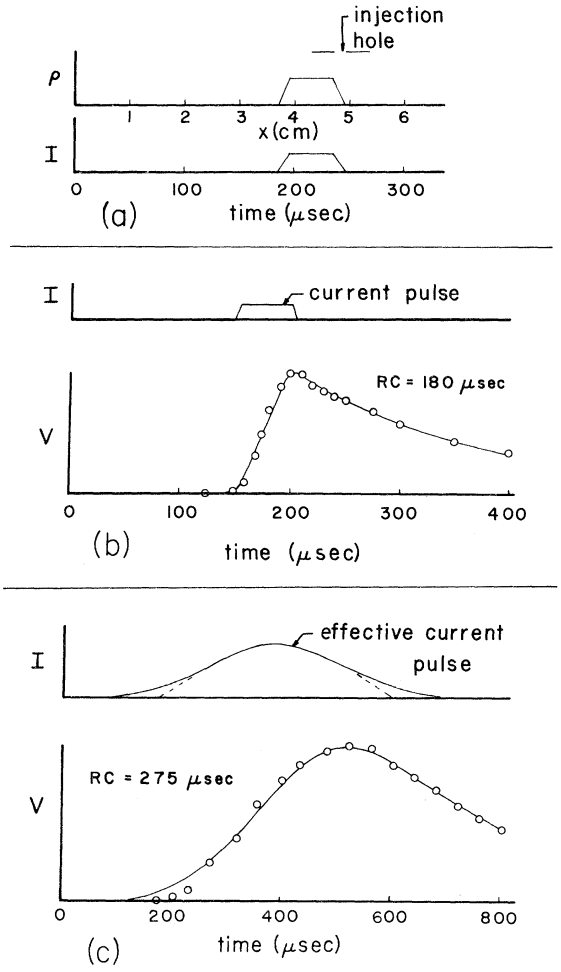

FIG. 6. Input and output pulses for the mobility cell. In (a) the spatial charge density ρ is shown for a 50-μsec pulse, injected through a 0.2 hole. The corresponding time dependence of the resulting current pulse is also shown. In (b) the output response to such a pulse is shown for $\tau \ll RC$. In (c) the response to a broadened pulse is given where the effective current pulse is assumed to be a Gaussian-broadened 100-μsec pulse. In (b) and (c) the solid lines are calculations based on the given current pulse and the open circles are taken from experimental data similar to the inset in Fig. 7.

order 0.1–1 mV/cm. This field is insignificant compared to the values of the applied drift field and does not contribute significantly to pulse broadening. Also the space charge field perpendicular to the surface is much less than 0.1 V/cm for this charge distribution and therefore, is negligible compared to the applied field.

2. *Pulse detection, Unbroadened pulses*

The shape of the voltage pulse obtained from the electrometer depends on the shape of the input current pulse, the pulse length τ, and the RC time constant of the detector. With the very large input impedance of the MOSFET source follower, the effective circuit consists of the input resistor R and the capacitance C of the collector plate connected in parallel. The response of this circuit is determined by the equation

$$RI_{\text{in}}(t) = V + RC\frac{dV}{dt}, \tag{10}$$

where I_{in} is the current pulse of electrons and V is the voltage across C. For simple pulse shapes this can be solved analytically; however, for more complicated pulse shapes, the output was calculated on a computer using the difference equation

$$V_{i+1} = V_i(1 - \Delta t/RC) + RI_{\text{in}}(t)\Delta t/RC, \tag{11}$$

where Δt is the step in time between V_{i+1} and V_i. The solutions obtained on the computer were compared with analytic solutions for special cases to make sure that problems of convergence did not exist.

Most of the data were taken in the regime in which the pulse length τ was $\ll RC$. An example of such a pulse is given in Fig. 6(b). In this figure, the solid line is the calculated response and the circles are points from the experimental pulse. These results show that the calculated response agrees very well with the data and indicates that the pulse of current corresponds to the *rising part* of the detected voltage—from the leading edge to the peak.

For many of the measurements, the pulse length was kept constant and the shape of the output-voltage pulse remained the same for electrons injected from either electron source. Consequently, for such data, the differential-time measurement could be obtained using either the peaks or the leading edges of the pulses to indicate the arrival times. For measurements in which different pulse lengths were used for the far and near sources, the transit time for the center of each pulse was determined.

The time constant of the electrometer circuit varied with temperature, between 150 and 275 μsec primarily as a result of the temperature dependence of R. This large value of RC was in fact very useful since when $\tau \ll RC$, the back edge of the current pulse is more accurately determined from the peak of the output voltage than for the case $\tau \approx RC$.

3. *Pulse detection—Broadened pulses*

For most measurements the current pulse width determined from the output voltage remained essentially constant and the analysis of the data was

straightforward as outlined above. However, when the tilt angle was decreased below approximately 10–12 mrad the pulse width, as determined from the response of the output voltage, suddenly and very rapidly started to increase, and for example, increased from 100 to about 300 μsec when θ was reduced to 7 mrad. This unusually rapid increase in the apparent width of the pulse cannot be explained by diffusion or broadening by the small fields at the edge of the current pulse. However, it can be well explained if one includes a small vibration of the apparatus and/or a sloshing mode of the liquid helium with an angular amplitude of order 1 mrad. Such a small vibration could easily be started while tilting the cell, or bumping the apparatus, etc., and is essentially undetectable by eye. This results in a slow modulation of the drift field of the form

$$F_D = E_\perp(\theta + \theta_V), \quad \theta_V = \theta_{V_0}\cos\omega t, \tag{12}$$

where θ_{V_0} is the amplitude of the vibration and in general also varies slowly with time, and ω is the vibration frequency. The period of these vibrations is expected to be longer than 10^{-2} sec and consequently, for times of flight which typically last (at the lower temperatures) less than 600 μsec, the surface is approximate stationary during the flight of a single pulse. Now as θ_V varies, some pulses have a larger drift field and arrive earlier than the average, while other pulses for which θ_V is negative, will arrive much later. When an average over 10^3–10^4 of these pulses is taken, the effective pulse is greatly smeared out. However, if θ_V is small (i.e., $\theta_V/\theta \ll 1$), the effective current pulse should be symmetrically broadened about $t_c = L/\mu F_\perp\theta$, since the time of flight at a particular value of θ_V is given by

$$t = \frac{L}{\mu F_D} = \frac{L}{\mu F_\perp(\theta + \theta_V)} \simeq \frac{L}{\mu F_\perp \theta}\left(1 - \frac{\theta_V}{\theta}\right). \tag{13}$$

In our analysis of the data we assumed such a symmetric broadening,[33] and were able to fit the observed pulse quite well as shown in Fig. 6(c). Generally we assumed the broadened pulse to be a Gaussian; although a truncated Gaussian, as indicated by the dotted lines in Fig. 6(c), fit the data somewhat better. This analysis showed that the center of the original pulse was near but not exactly at the midpoint between the start of the voltage pulse and its peak. Small corrections [typically (5–20)%] were made to include this shift. The drift velocities obtained from this analysis agreed very well with data taken at large angles, indicating a consistent determination of the pulse position at various electric fields.

V. EXPERIMENTAL RESULTS

A plot of the drift velocity versus drift field is shown for two different temperatures in Fig. 7. Each point is the differential result of two transit time measurements, one for each source. A typical pair of pulses are shown in the insert. In Fig. 7(a), no non-Ohmic behavior occurs, and the mobility is determined by the slope of the graph. However, at lower temperatures heating effects similar to those reported in Ref. 4 were observed, as is seen in Fig. 7(b). Nevertheless, it was always possible to obtain at least three to four data points in the low-field region of linear behavior

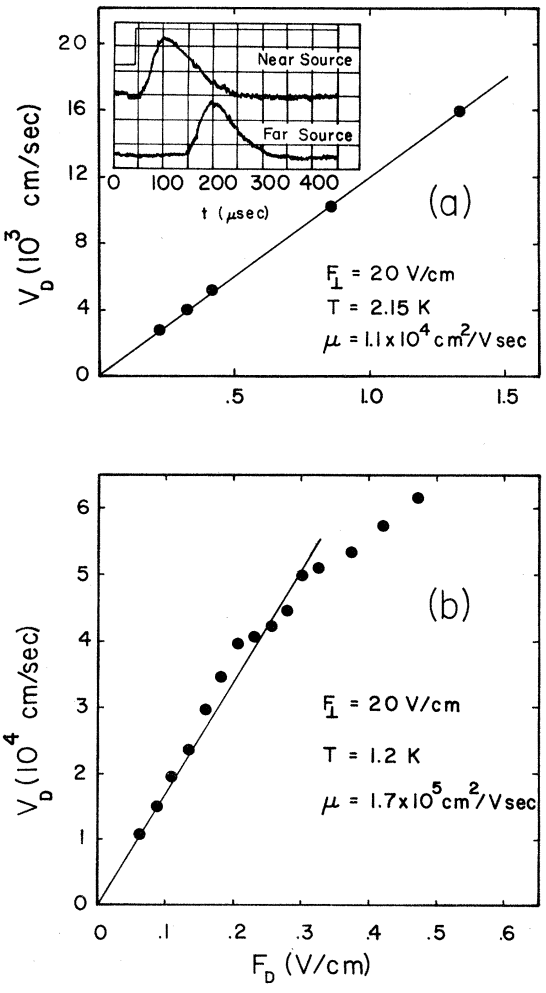

FIG. 7. Two plots of drift velocity vs drift field taken at 2.15 and at 1.2 K, with $F_\perp = 20$ V/cm in both cases. The inset shows the oscilloscope trace for a typical time of flight measurement at 1.2 K. The top trace shows the electron source gate pulse, which also triggers the detection electronics. The middle trace shows an averaged electron pulse arriving from the source farthest from the collector.

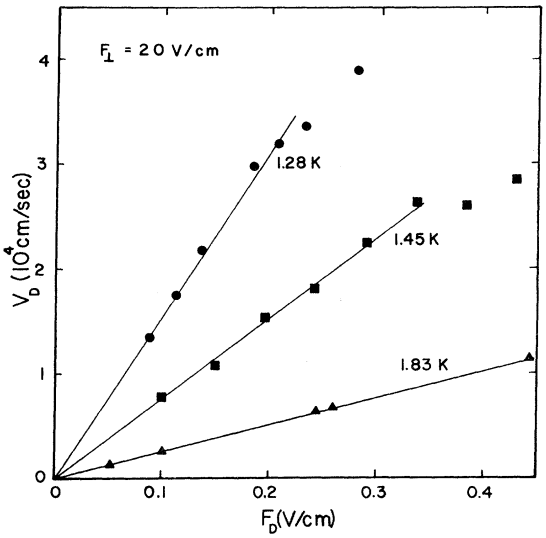

FIG. 8. Plots of drift velocity vs drift field taken at several different temperatures, with $F_\perp = 20$ V/cm in all cases.

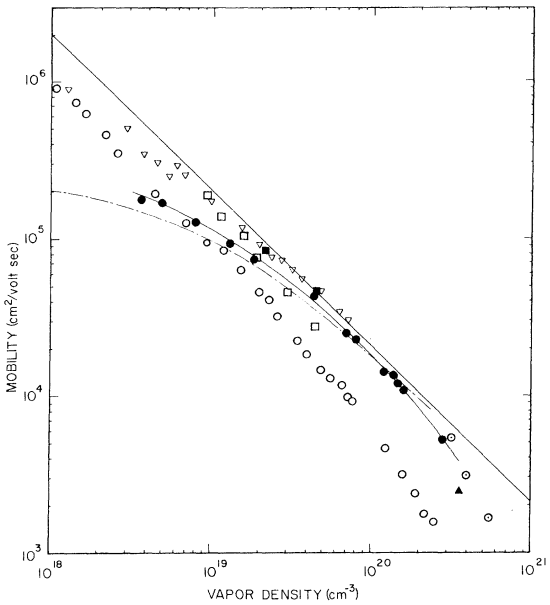

FIG. 9. Mobility vs vapor-density plot showing theoretical curves, previous experimental results and results of the present experiment. ——, two-dimensional vapor scattering; – – –, Cole's calculation (Ref. 8). ▽, Rybalko *et al.* (Ref. 12); ▲, Ostermeier and Schwarz (Ref. 4); □, Brown and Grimes (Ref. 6); ■, Rybalko and Kovdrya (Ref. 7); ○, Sommer and Tanner (Ref. 5); ⊙, Levine and Sanders (Ref. 34); ●, present work.

(see Sec. V C) and in such cases the mobility was determined by the linear region of the curve. Additional measurements of drift velocity versus drift field are presented in Fig. 8.

A. Ohmic (linear) regime

1. Low holding fields

Figure 9 is a plot of the mobility versus vapor density for $F_\perp = 20$ V/cm, with each point determined from the low-drift-field region (see Figs. 7 and 8). Theoretical curves and previously reported data are also displayed for comparison. At high density, our data agree with vapor mobility measurements.[34] In the middle range, we agree with semiclassical two-dimensional kinetic theory for vapor-atom limited scattering, as does the data of several other investigators.[6,7,12] Below $n = 2 \times 10^{19}$ cm^{-3}, the mobility begins to level off in the manner predicted by Cole.[2]

We interpret the leveling off of the mobility at low-vapor densities as evidence for the presence of the electron-ripplon scattering process. At a vapor density of 5×10^{18} cm^{-3}, the mobility is depressed by a factor of 2.3 (from the value expected for only vapor-atom scattering) indicating that at this density, the electron-ripplon interaction is, in fact, the dominant scattering mechanism. Since the main contribution to the mobility from ripplon scattering arises from the relatively short-wavelength surface-tension capillary wave (gravity waves are unimportant), our measurements are evidence of an electron-ripplon interaction in the *capillary-wave regime*.

The overall depression of the mobility below $n = 2 \times 10^{19}$ cm^{-3} is in fairly good agreement with the theoretical predictions of Cole.[8] A small but reproducible discrepancy does exist however; the experimental mobility is (20–30)% higher than Cole's theoretical prediction. This shift could arise in a number of ways; for example, from small changes in the dielectric constant at the surface, or from small changes in the values of the surface tension. However, if we assume that the difference between experiment and theory is primarily the result of the neglect of the surface term in the scattering matrix element,[18] then we can use our data to obtain information about the nature of the potential at the surface—i.e., we use our data to determine R.

To analyze the data in this way we recalculated the mobility as a function of the parameter R, using Eq. (5). Since the matrix elements depend sensitively on the value of the effective charge Q, we have used the recent accurate value[35] of the dielectric constant $\epsilon = 1.0572$ to obtain $Q = 6.95 \times 10^{-3}$. We have also used the recent measurements of the surface tension[19,20] to include the weak temperature dependence of this parameter in μ. The use of these values gives a slightly lower theoretical value for the ripplon-limited mobility than that obtained by Cole (in the limit $R \to \infty$).

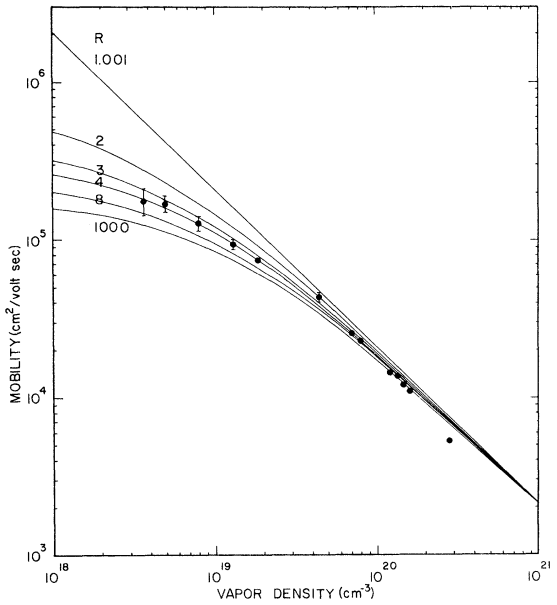

FIG. 10. Mobility vs vapor-density data from the present experiment and theoretical curves after Gaspari and Bridges (Ref. 18) with several different values of the ratio parameter R.

The results of these calculations are shown in Fig. 10 along with our data. It is interesting to note that the experimental mobility generally follows close to the curve for $R=4$. The fact that the data does not cross over a wide range of R supports our suggestion that the discrepancy between the earlier theory and our data is the neglect of the surface term. From this data we obtain $R=3.75\pm1.0$.

Once R is known, we are in a position to estimate the parameter b in the surface potential model of Cole[2] (Sec. II A). For this model the relationship between R and b is given by[18]

$$R=(1+\alpha b)^2/(\alpha b)^2, \quad \alpha=(2mV_0)^{1/2}\hbar. \tag{14}$$

We have plotted R in Fig. 11 as a function of b assuming a step potential V_0 of 1 eV at the liquid surface. Using the experimental range of R (indicated by the shaded region) we obtain $1.7<b<2.9$ Å. Although generally smaller than the interatomic spacing (3.6 Å) this range of b is very reasonable and lends further support to our interpretation. Since however, the value of b is model dependent, we note that the more important parameter is R.

2. *Large holding fields*

Although we could not make measurements as a function of $F_\perp$ at the lowest temperatures, and thus check Shikin's predictions,[9] we were able to investigate the perpendicular field dependence at higher temperatures. At 2.07 K (vapor density

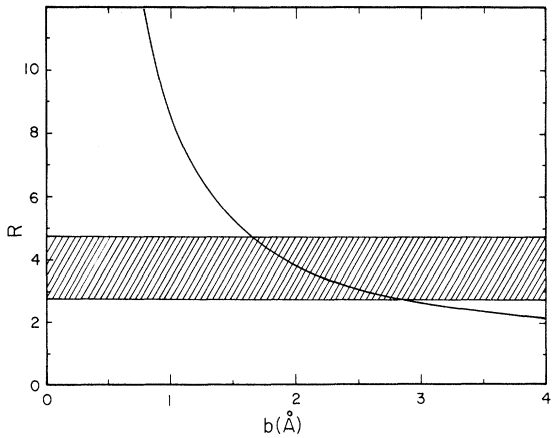

FIG. 11. Plot of R vs b for the potential model of Cole (Ref. 2). The step potential at the surface is assumed to be 1 eV. The experimentally observed range of R is shown as a shaded band.

$=1.4\times10^{20}$ cm^{-3}), the mobility was measured at different values of the perpendicular electric field from 20 to 120 V/cm. For this temperature, the mobility is determined primarily by electron-vapor scattering. Within a given run the error was about 5%, and from one run to another the spread was within ±10%. No change in mobility was observed. This indicates that the electrons are in the hydrogeniclike states and not in a potential well formed by the perpendicular field. In the latter case, the mobility would have an observable dependence on the perpendicular field. For electrons in hydrogenic states, the first-order correction to the mobility arising from a perpendicular field between 20 and 120 V/cm is negligible compared to our errors.

B. Non-Ohmic (hot electron) regime

1. *General features*

Figure 12 shows several plots of the mobility as a function of the drift field at $F_\perp=20$ V/cm. These data are analyzed completely and varies slightly from our preliminary results which were used by Crandall.[28] The major features for all curves is the decrease of the mobility at high-drift fields at all temperatures. At the lowest temperature the mobility is constant at low-drift fields, then *increases* slightly before starting the monotonic decrease observed at high fields. Such behavior is expected[28] in the regime where both ripplon and vapor-atom scattering are present. However, the bump in the curve is smaller than the theoretical prediction based on lowest-order perturbation theory.[36]

The monotonic decrease of μ at high-drift field is attributed to a heating of the electron gas and a

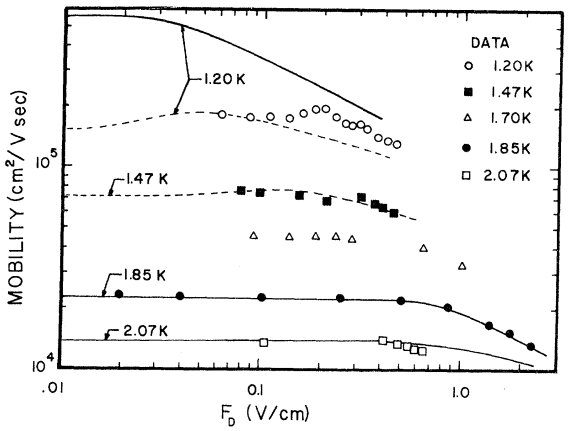

FIG. 12. Several plots of mobility vs drift field showing data from the present experiment and theoretical curves of Crandall (Ref. 28). The solid lines are for the electron-vapor scattering mechanism alone while the dashed lines included a phenomenological surface scattering term.

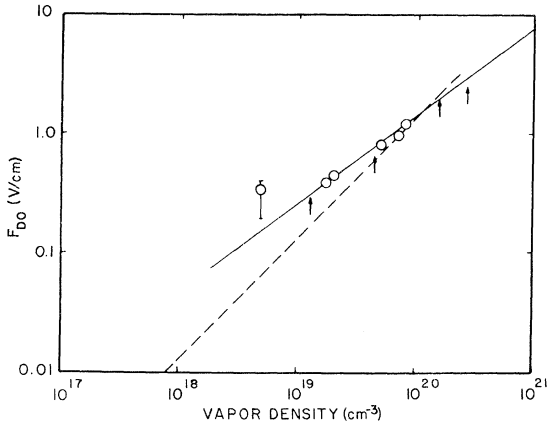

FIG. 13. Plot of the onset field F_{DO} as a function of the vapor density. The circles represent data which extends well into the nonlinear range. The arrows are lower estimates from data which extends only a short way into the nonlinear regime. The dashed line is an estimate of F_{DO} from Crandall's calculations (Ref. 28) assuming only electron-vapor atom scattering is present. $F_{\perp}=20$ V/cm.

consequent population of the higher hydrogeniclike levels. Since the scattering mechanism for the upper levels is predominantly via electron–vapor-atom collisions, the net relaxation rate is a weighed average of the scattering in many energy levels. The reason for the increase in the scattering rate was first pointed out by Crandall[28] to be a density-of-states effect as discussed in Sec. II B2. Although the matrix element decreases as the electrons move to higher hydrogeniclike states, the density of final states for the scattering process increases more rapidly and the net scattering time is thereby shortened.

At the higher temperatures ($T \geq 1.85$ K), the entire mobility curve is well described using only the electron–vapor-atom scattering mechanism. The theoretical curves obtained by Crandall[28] for this regime fit the data (Fig. 12) surprisingly well considering there are no adjustable parameters. At the lower temperatures the mobility calculated assuming only electron–vapor-atom scattering, is too high, indicating that another mechanism—electron-ripplon scattering—is present (see Sec. IV A). Crandall used a phenomenological energy- and temperature-independent matrix element to represent this additional scattering process in the lower temperature regime. This is represented by the dashed line in Fig. 12 and is in fair agreement with the data overall. However, to fit the *shape* of the curve, a better model for the electron-ripplon scattering process is clearly needed.

2. *Onset of nonlinear effects*

From Fig. 12, the onset of nonlinear effects occurs at lower electric fields when the temperature is lowered. To show this more clearly, we define an onset parameter F_{DO} to be the drift field at which the mobility deviates 20% from linearity (where the subscript DO indicates deviation onset). Although not a well-defined parameter theoretically, it is useful in describing how the onset of nonlinear behavior changes with density and temperature. In Fig. 13 we have plotted F_{DO} as a function of vapor density n. Here the circles are from data which extend well into the nonlinear range, while the arrows are lower limit estimates from other data.

The observed increase of F_{DO} with vapor concentration is expected since the mean free path λ for the electron varies as n^{-1}. Although the curve in Fig. 13 has a slope of 0.75 rather than 1.0, the general trend is as expected, and one might attribute the difference in the slopes to the imprecise definition of F_{DO}. However, a similar determination of F_{DO} obtained from Crandall's theoretical curves for vapor-atom scattering (solid lines in Fig. 12) *does* give a slope close to 1.0 and lies below our experimental curve for $n < 8\times 10^{19}$ cm^{-3} as shown in Fig. 13. The observed slower decrease of F_{DO} with n is therefore interpreted as additional evidence that the ripplon-scattering process is becoming important. We expect that at low densities where the vapor scattering process becomes negligible, F_{DO} will be relatively independent of n. The data point for 5×10^{18} cm^{-3} clearly indicates this trend but is perhaps ambiguous because of the bump in the mobility curve.

The variation of F_{DO} with n also serves as a check that our low-temperature data always had

some points in the linear regime. Extrapolating the data at higher densities down to 5×10^{18} cm^{-3} ($T=1.2$ K) indicates that heating effects become appreciable above 150 mV/cm. Since our drift field at this density extends down to 60 mV/cm, we clearly have some data in the linear regime. Our measurement of F_{DO} at this density is considerably higher than this extrapolation as indicated in the figure.

A further extension (a perhaps questionable extrapolation) of the theoretical curve obtained from Crandall's work down to $n=10^{17}$ cm^{-3}, the density at which the mobility levels off in the work of Grimes and Adams,[10] indicates that heating effects would be important above 1 mV/cm. This is more than an order of magnitude smaller than the drift fields at which nonlinear effects were observed in the plasma studies and may be a further indication that the different experiments are, in fact, measuring different quantities.

Finally, we note that the onset of non-Ohmic behavior is also dependent upon the perpendicular field in a qualitatively understandable way. At 2.07 K the onset occurs at 0.48 V/cm for $F_\perp=20$ V/cm and at 2.3 V/cm for $F_\perp=120$ V/cm. At this temperature the non-Ohmic behavior results from scattering into higher hydrogenic states.[28] Since the spacing between energy levels increases with the holding field, the scattering into higher states at large holding fields requires more energy. Therefore, it is expected that the drift field at which the onset occurs, will increase with the holding field.

VI. DISCUSSIONS AND CONCLUSIONS

The time-of-flight mobility measurements presented above generally agree well with previous experimental data for $n>4\times10^{19}$ cm^{-3} particularly with the other time-of-flight experiments, and provide additional evidence for the two-dimensional nature of electrons on the surface of liquid helium. From 4×10^{19}–2×10^{20} cm^{-3}, the experimental mobility lies very close to the theoretical calculations based on the electron–vapor-atom scattering interaction, while at higher densities the mobility falls below the two-dimensional curve. This depression of the mobility at high densities agrees well with the earlier work of Levine and Sanders,[34] and has been explained by the formation of electron bubble states in the high-density vapor.

In all of these measurements the observations have been internally self-consistent. At the higher drift fields (larger tilt angles), the pulse length determined by the output voltage pulse agrees very well with the measured input parameters, and the calculated shape of the output pulse also agrees well with experiment. At lower tilt angles, the voltage pulse widths suddenly and rapidly started to increase as the tilt angle decreased. This was found to be the result of small-amplitude vibrations of the apparatus or sloshing modes of the helium plus the fact that the output voltage pulse is an average over 10^3–10^4 pulses. When this effect is included, the calculated pulses agree well with the observations and moreover, the drift times obtained with the broadened pulses agree very well with the data at larger angles. Thus, we believe that our interpretation of the pulse broadening is correct and that this method of analysis can be applied to the data at lower temperatures.[37]

In addition to showing the self-consistency of these measurements, the above analysis also indicates the difficulties in extending the time-of-flight measurements to lower-drift fields and/or larger-perpendicular fields. For perpendicular fields of order 10–20 V/cm, an order of magnitude decrease in the vibration amplitudes would extend the available drift fields down to 5 mV/cm and provide a larger range for measurements in the linear regime. However, for perpendicular fields of 100–1000 V/cm and low-drift fields, the required vibration isolation may be very difficult to achieve.

At vapor densities below 4×10^{19} cm^{-3} our measurements of the mobility again fall below the theoretical two-dimensional curve in a manner similar to the predictions of Cole, and are interpreted as evidence for the electron-ripplon interaction. Additional evidence for this interaction is also inferred from the vapor density dependence of the drift electric field at which nonlinear effects become important as in Sec. V B 2. However, the experimental situation is far from clear, since the various experiments which provide evidence for the electron-ripplon interaction yield values for the ripplon-limited mobility that range over a factor of 50. The mobility obtained by Grimes and Adams[10] from the plasma linewidths is about 2×10^7 cm^2/V sec, that obtained by Rybalko *et al.*,[12] from ac power absorption measurements is about 3–4×10^6 cm^2/V sec while the mobility we have measured appears to be approaching a value of 4–6×10^5 cm^2/V sec.

The difference between these results is not yet understood but likely arises from a combination of different factors. First, different experiments have measured different quantities: the plasma lifetime, the ac losses of electrons moving back and forth on the surface, the phase shift in an ac signal, and the drift velocity of electrons moving in a dc drift field. These are not necessarily equivalent and may involve different averages of the momentum relaxation rate. Further, other

considerations which have not yet been dealt with may also enter the picture. For example, surface waves generated by external vibrations and thermally generated plasma waves are clearly present. Do they contribute significantly to the various measurements and are they more important in one experiment than another? Certainly the observation that the onset of nonlinear effects in two experiments (Sec. V B 2) varies by different amounts from a theoretical extrapolation, supports the assumption that other factors must be included.

Second, the parameters used in different experiments vary considerably. One parameter that varies widely is the surface-charge density n and furthermore, the larger the electron density, the larger the limiting value of the mobility. Grimes and Adams used densities between 10^6–10^9 cm^{-2}, Sommer and Tanner used densities of order 10^7 cm^{-2}, Rybalko *et al.* used densities between 10^5–10^6 cm^{-2}, while the present measurements used densities less than 10^4 cm^{-2}. As discussed earlier, when large densities are present, the assumption of a free-electron gas model becomes a poor approximation and the systematic increase in mobility with density may be real. However, this factor alone probably cannot account for all the discrepancies either since both Grimes and Adams and Rybalko *et al.*, took measurements near $n \simeq 10^6$ cm^{-3}. The present measurements, with $n < 10^4$ cm^{-3}, come closest to the approximations in the theory, and in this regard might be expected to give better agreement with the calculations than the high-density data. The study of the low-drift field mobility is clearly not yet understood and additional work, both theoretical and experimental, is needed to clarify various situations.

Finally, in the high-drift field regime we have observed nonlinear effects in the mobility. At the higher densities, this is primarily a monatonic decrease in μ as a function of F_D while at low densities ($n = 5 \times 10^{18}$ cm^{-3}) the mobility first increases with F_D before starting a monotonic decrease. The high-temperature results have been explained by Crandall in terms of electron–vapor-atom scattering in excited states. However, in the regime in which the electron-ripplon interaction is dominant much remains to be explained.

ACKNOWLEDGMENTS

We wish to thank George Gaspari for many helpful discussions on the theoretical aspects of this problem. We also thank C. C. Grimes and T. Brown for discussions concerning their measurements and other experimental considerations, and R. Crandall for helpful discussions concerning the nonlinear regime.

---

*Project supported in part by the Research Corp. and in part by a University of California Faculty Research Grant.

†Research supported by the NSF.

‡Present address: Culler/Harrison, Inc., Goleta, Calif. 93107.

[1]W. T. Sommer, Ph.D. thesis (Stanford University, 1964) (unpublished).

[2]M. W. Cole, Phys. Rev. B 2, 4239 (1970); M. W. Cole and M. H. Cohen, Phys. Rev. Lett. 23, 1238 (1969).

[3]C. C. Grimes and T. R. Brown, Phys. Rev. Lett. 32, 280 (1974).

[4]R. M. Ostermeier and K. W. Schwarz, Phys. Rev. Lett. 29, 25 (1972).

[5]W. T. Sommer and D. J. Tanner, Phys. Rev. Lett. 27, 1345 (1971).

[6]T. R. Brown and C. C. Grimes, Phys. Rev. Lett. 29, 1233 (1972).

[7]A. S. Rybalko and Yu. Z. Kovdrya, J. Low Temp. Phys. 18, 219 (1975).

[8]M. W. Cole, Rev. Mod. Phys. 46, 451 (1974).

[9]V. B. Shikin, Sov. Phys.-JETP 33, 387 (1971).

[10]C. C. Grimes and G. Adams, Phys. Rev. Lett. 36, 145 (1975).

[11]P. Platzman and G. Beni, Phys. Rev. Lett. 36, 626 (1976).

[12]A. S. Rybalko, Yu. Z. Kovdrya, and B. N. Esel'son, JETP Lett. 22, 569 (1975).

[13]Preliminary results were presented earlier. J. McGill and F. Bridges, Bull. Am. Phys. Soc. 19, 284 (1974).

[14]H. Huang, Y. Shih, and C. Woo, J. Low Temp. Phys. 14, 413 (1973).

[15]M. A. Woolf and G. W. Rayfield, Phys. Rev. Lett. 15, 235 (1965).

[16]R. Crandall, Phys. Rev. A 6, 790 (1972).

[17]V. B. Shikin and Yu. P. Monarkha, J. Low Temp. Phys. 16, 193 (1974).

[18]G. Gaspari and F. Bridges, J. Low Temp. Phys. 21, 535 (1975).

[19]S. T. Boldarev and V. P. Peshkov, Physica (Utr.) 69, 141 (1973).

[20]K. N. Zinov'eva and S. T. Boldarev, Sov. Phys.-JETP 56, 1089 (1969).

[21]V. B. Shikin and Yu. P. Monarkha, Sov. Phys.-JETP 38, 373 (1974).

[22]R. S. Crandall and R. Williams, Phys. Lett. A 34, 404 (1971).

[23]R. S. Crandall, Phys. Rev. A 10, 1370 (1974).

[24]P. M. Platzman and H. Fukuyama, Phys. Rev. B 10, 3150 (1974).

[25]R. W. Hockney and T. R. Brown, J. Phys. C 8, 1813 (1975).

[26]R. S. Crandall and R. Williams, Phys. Rev. A 5, 2183 (1972).

[27]R. S. Crandall, Phys. Rev. A 6, 790 (1972).

[28]R. S. Crandall, Phys. Rev. B 12, 119 (1975).

[29]R. Williams, R. S. Crandall, and A. Willis, Phys. Rev. Lett. 26, 7 (1971).

[30]C. C. Grimes (private communication). The measured mobility from the plasma linewidths is independent of temperature within the experimental error (20%) over the range 0.48–0.7 K.

[31]In the region between the electron sources, the axial fringe-field component along the surface F_f was calculated using a conformal map. For a given applied perpendicular field $F_\perp$ we find $F_f/F_\perp < 10^{-4}$.

[32]This will be true when the electrons injected at the beginning of the pulse have a large enough drift velocity that they move a distance > 0.2 cm during the length of the pulse. When the drift velocities are very low, this condition is no longer met and the ramp section will be less than 0.2 cm.

[33]A rough estimate of the shape of the effective pulse can be obtained by using Eq. (11) to calculate I_{in} from the experimental voltage pulse. However, the results of this calculation are very noisy since the value of dV/dt is required.

[34]J. L. Levine and T. M. Sanders, Jr., Phys. Rev. 154, 138 (1967).

[35]R. F. Harris-Lowe and K. A. Smee, Phys. Rev. A 2, 158 (1970).

[36]R. S. Crandall (private communication).

[37]Other corrections, such as the effects of the nonlinearity in the μ-vs $-F_D$ curve on the effective pulse-broadening and second-order terms in θ_v [see Eq. (13)], have also been considered, but the net correction from these factors is within our experimental errors.